Effects of diffuse cracking around a main cohesive crack in diagonal splitting tests

I.Arbilla & J.Planas
Dpto. de Ciencia de Materiales, ETSI Caminos, UPM, Madrid, Spain

ABSTRACT: The cohesive crack model is a relatively simple and accurate means of describing fracture in concrete and other quasibrittle materials. In its standard application, it is assumed that all the material surrounding the cohesive crack remains linear elastic. However, detailed analyses show that the tensile strength is exceeded within the supposedly elastic region, which means that secondary cracking must occur. This paper briefly summarizes the basic features of a simple extension of the cohesive crack to include secondary cracking. It also discusses previous computations for unnotched beams subjected to three-point-bend beams, and explores the effect of secondary cracking on the results of the diagonal splitting test (Brazilian test). Various specimen sizes and two load-bearing-strip widths are considered. In particular, the influence of the peak load and the map of secondary crack density are analyzed.

1 INTRODUCTION

The cohesive crack model, first proposed by Barenblatt (1962) and Dugdale (1960), in very specific contexts, was later extended by Hillerborg (1976) to become a general approach to the fracture of concrete in tension. The model has proved to be relatively simple and efficient to describe the fracture of concrete and other quasibrittle materials, at least in the cases were failure occurs through a single crack or a set of discrete cracks.

One of the simplifications usually included in the cohesive crack model is that all nonlinear behavior is localized into the cohesive zone while the material surrounding the crack remains linear elastic. Although this hypothesis is not conceptually necessary (Elices & Planas 1989; Bazant & Planas 1998), it makes much simpler both theoretical and numerical analyses of cohesive crack problems and became a basic ingredient of the standard formulation.

A limitation of the standard formulation of the cohesive crack model is that it leads to solutions that contradict one of the basic hypotheses of the model, namely, that a cohesive crack forms in at a formerly elastic point when the stress reaches the tensile strength f_t. Indeed, in most of the solutions of single cohesive crack problems, more or less large regions have been found in the supposedly elastic bulk material where the tensile strength is exceeded. For example, in Figure 1, a small but finite region over which the largest principal stress exceeds the tensile strength is found around the cohesive crack tip in a three-point-

bend specimen in which a cohesive crack is made to grow in mode I from a relatively deep notch (Guinea 1990; Planas et al. 1992).
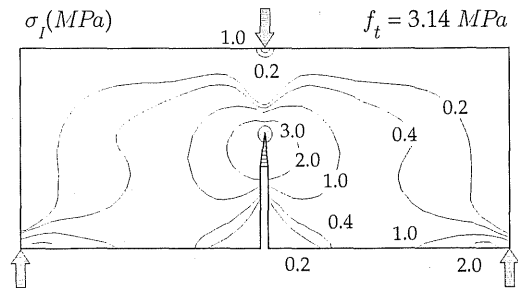

Figure 1: Maximum load isostress lines for first and third principal stresses (Planas et al., 1993).

For unnotched three-point-bend specimens it has been long foreshadowed that the standard solution involved stresses exceeding the tensile strength over allegedly elastic regions. This point was quantitatively demonstrated by Olsen (1994), some of whose results are compiled in Figure 2. It shows a large area over which the tensile strength is exceeded.

$f_t = 4.00\ MPa$

$D/2$

σ

$D/2$

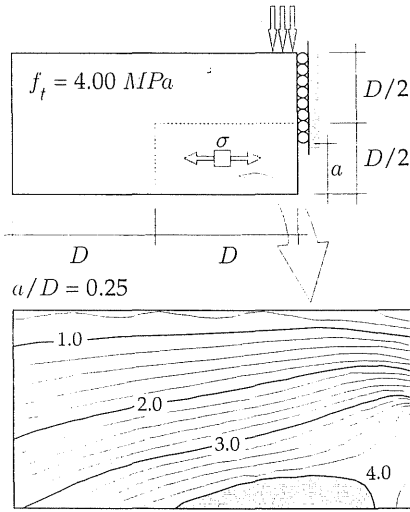a

D D

$a/D = 0.25$

1.0
2.0
3.0
4.0

Figure 2: Isolines of horizontal normal stress in a three-point-bend unnotched beam for $a/D = 0.25$ relative depth of the cohesive zone. The tensile strength f_t is exceeded over the gray shadowed regions (Olsen, 1994).

The foregoing facts imply the following three consequences:

- The standard approach to the cohesive crack model leads to inconsistent solutions whose accuracy needs to be assessed trough a higher level model.

- According to the cohesive crack model itself, secondary cracking must occur in the regions where the tensile strength is exceeded.

- A higher-order model is needed that, preserving the main concepts of the cohesive crack model, relieve the inconsistency and adequately describe the secondary cracking.

This work presents one of the many possible higher order models and describes the results of its application to the diagonal splitting test.

2   DIFFUSE CRACK MODEL

The diffuse crack model developed in this work is a three–dimensional generalization of the unidimensional model proposed by Planas & Elices (1993) to describe shrinkage microcracking in concrete. Its starting point is the cohesive crack model which assumes the development of a crack perpendicular to the maximum principal stress when this reaches the tensile strength f_t. After the cohesive crack has formed,
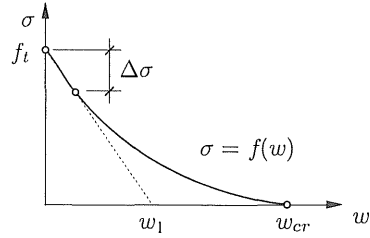

Figure 3: Generic softening stress-crack opening curve.

the stress transferred across its faces is given, for *monotonic* mode I crack opening, by a unique function of the crack opening w:

$$\sigma = f(w) \tag{1}$$

The $f(w)$ function is known as the softening function. Figure 3 shows the shape of this function for concrete.

The diffuse crack model adds to the basic cohesive crack model some complementary assumptions regarding crack kinematics. For simplicity, we first describe the uniaxial model and then give the generalization to three dimensions.

2.1   *Uniaxial model*

The core idea in the uniaxial model is that diffuse cracking can be described as a set of parallel cohesive cracks, spaced a relatively small distance s, in an otherwise elastic bar. If the cracks are close enough, we can describe their macroscopic effect as a distributed inelastic strain ε^p given by

$$\varepsilon^p = \frac{w}{s} \tag{2}$$

where w is the average crack opening. The uniaxial stress transferred through the crack set for monotonic inelastic stretching, directly derives from the softening curve (Eq. 1) as

$$\sigma = f\left(s\varepsilon^p\right) = f_s\left(\varepsilon^p\right) \tag{3}$$

where $f_s\left(\varepsilon^p\right)$ is a stress–inelastic curve which displays softening. If the crack spacing tends to zero, the softening rate also tends to vanish. Then the model displays a perfectly plastic behavior. If the first stretch of the softening curve is approximately linear (Fig. 3) the stress drop $\Delta\sigma$ is given by

$$\Delta\sigma = f_t \frac{s}{w_1}\varepsilon^p \tag{4}$$

484

For infinitely close cracks, $s \to 0$ and $\Delta\sigma \to 0$. Therefore, as long as monotonic stretching is concerned, the behavior tends to be perfectly plastic as the crack spacing is reduced.

The unloading behavior is also needed to complete the model because a main cohesive crack may develop and, as it grows, the zone of diffuse cracking may unload. Planas & Elices (1993), based of the results of other authors (Reinhardt 1984; Yankelevsky & Reinhardt 1987), justified that when a crack gets slightly open it does not close again upon unloading. We adopt here this result and assume that the inelastic strain $\bar{\varepsilon}^p$ is fully irrecoverable. This is formally identical to an elastic-plastic stress-strain behavior; perfectly plastic if $s = 0$ and plastic with softening if $s \neq 0$.

2.2 *Triaxial model*

The simplest way to generalize the former uniaxial model to three dimensions is to assume an elastoplastic behavior with Rankine criterion and associative flow rule. The corresponding equations are

$$\sigma = \mathbf{E}\left(\varepsilon - \varepsilon^{\mathbf{P}}\right) \qquad (5)$$

$$\sigma_1 - f_s\left(\bar{\varepsilon}^p\right) = 0 \qquad (6)$$

$$d\varepsilon^p = \mathbf{P}_1\, d\bar{\varepsilon}^p \qquad (7)$$

where σ = stress tensor; $\mathbf{E}$ = fourth-order elastic tensor; ε = strain tensor; ε^p = inelastic strain tensor; σ_1 = maximum principal stress; $\bar{\varepsilon}^p$ = equivalent inelastic strain; and $\mathbf{P}_1$ = projector of the stress tensor on the direction of its first principal stress. The function $f_s\left(\bar{\varepsilon}^p\right)$ is identical to that defined for the uniaxial model by Equation (3).

The equivalent inelastic strain $\bar{\varepsilon}^p$ gives global information about the softening process in each point of the bulk material. It characterizes the maximum crack opening average of every crack developed in a point and does not take into account the orientation of each crack. The equivalent inelastic strain equals the uniaxial inelastic strain if the unidimensional case is considered, as it is followed from Equation (7).

3 NUMERICAL ANALYSIS

This analysis shows the influence of diffuse cracking on the predicted behavior of three point bend and diagonal splitting test specimens. The numerical analysis makes use of ABAQUS, a finite elements commercial code.

The main crack is simulated by softening spring elements located along the central cross section. The diffuse cracking is modeled defining an elastoplastic material behavior (according to former section) for the bulk material. Nor ABAQUS nor any other com-
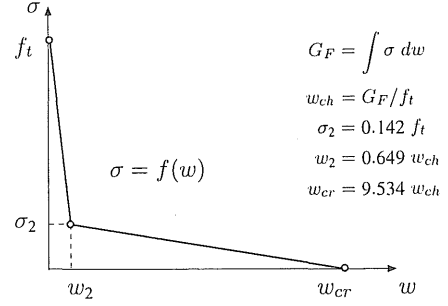

Figure 4: Softening curve used in calculations (Rocco 1996).

mercial finite element code support any material behaviour with Rankine first principal stress yield criterion and associative flow rule. That's why it is necessary to develop an user material subroutine (UMAT in ABAQUS nomenclature) to make use of this kind of material.

The subroutine implements a two dimensional plane stress model. The plastic softening function $f_s\left(\bar{\varepsilon}^p\right)$ is a polygonal derived from the cohesive softening function and the value of the average distance between consecutive diffuse cracks (Eq. 3).

The softening curve used in all the calculations (Fig. 4) corresponds to a microconcrete tested in the authors laboratory (Rocco 1996).

3.1 *Three point bend beams*

The finite element mesh models the right half of an unnotched beam. The span to depth ratio is four. The calculations consider five beam depths, scaled according to the ratios $1:2:4:8:16$. Detailed information about the mesh can be found in Arbilla et al. (Arbilla et al. 2000).

3.2 *Diagonal splitting test specimens*

The finite element mesh, a square pattern made up by 64×64 elements, models only the upper right quarter of the specimen because of the symmetry conditions of the test. The side of each element is $D/128$, where D = test specimen height.

The calculations consider six sizes of specimens and two widths of bearing strips. The sizes are scaled according to the ratios $1:2:4:8:16:32$.

3.3 Calculations

Three different calculations are performed for each unnotched three-point-bend beam:

- Standard cohesive crack model: main cohesive crack running through elastic material.

485

- Nonsoftening diffuse cracking: main cohesive crack running through a material with infinitely close diffuse cracks(crack spacing $s = 0$).

- Softening diffuse cracking: main cohesive crack running trough a material with diffuse softening cracks corresponding to an assumed minimum crack spacing identical to the finite element size. This means that only one crack can develop in each element.

Only the first and the third calculations are performed for each splitting test specimen because we are looking for secondary localized cracks.

4 RESULTS

The results are shown in dimensionless form, so they are useful not only for the particular microconcrete considered here, but also for any other material with a softening function of identical shape.

Loads are referred to the nominal peak load for elastic brittle–behavior. Geometric dimensions are referred to the characteristic length of the microconcrete l_{ch}, defined as

$$l_{ch} = \frac{E G_F}{f_t^2} \qquad (8)$$

where E = elastic modulus and G_F = fracture energy. The value of the characteristic length of the microconcrete is $l_{ch} = 122$ mm, whereas the value of an ordinary concrete $l_{ch} \approx 300$ mm.

Although equivalent inelastic strain is already a dimensionless variable, it is referred to the elastic strain corresponding to the tensile strength f_t.

4.1 *Unnotched three-point-bend beams*
One of the main results is that the diffuse crack model relieves the overstress appearing in the standard cohesive crack approach, so the stress nowhere exceeds the tensile strength. Of course, this is done at the expenses of inelastic strains appearing in the material. The inelastic strain concentrates in the small dark rectangle shown in Figure 5. The inelastic strain distribution inside that rectangle is shown in Figure 6 for various cases. For nonsoftening diffuse cracking, the inelastic strain is smoothly distributed, and more intense for small sizes (Fig. 6 a) than for large sizes (Fig. 6 b). For softening diffuse cracking the inelastic strain is again more intense for small size (Fig. 6 c) than for large sizes (Fig. 6 d). However, the inelastic strain distribution is less smooth and localization bands may be identified for small sizes (Fig. 6 c). This is the main difference between the two diffuse crack models.

The first consequence of the localization is that the maximum inelastic strain is about 5 times larger for the softening diffuse cracks. Although the existence of localization bands is numerically significant, its effect on experimental results is nil. In fact, the soften-
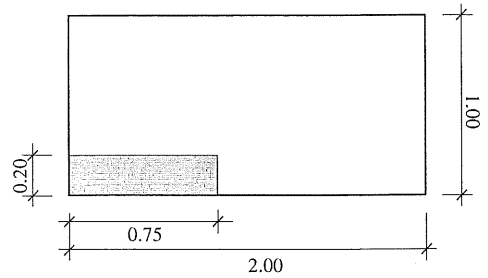

Figure 5: Right half of the specimen; the dark rectangle shows the zone where diffuse cracking takes place. All dimensions are referred to the beam depth.
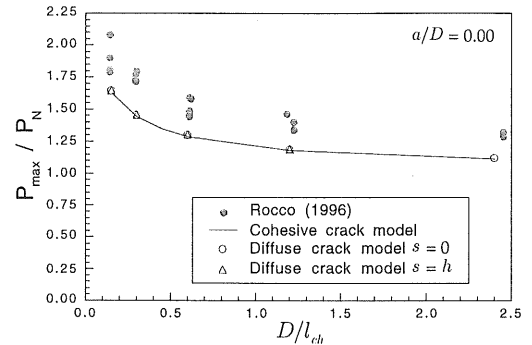

Figure 7: Peak load calculated with the cohesive crack model and the diffuse crack model and experimental results from Rocco(1996) for unnotched three-point-bend beams.

ing associated to the worst strain localization is less than 0.4% of f_t for all the investigated sizes. The corresponding (maximum) crack opening is $w \approx 0.1 \ \mu$m for a typical concrete with $G_F = 100$ N/m and $f_t = 3$ MPa. This means that the localization bands, which could be seen as isolated cracks, are virtually impossible to detect experimentally since their opening is in the submicron range.

Finally Figure 7 shows the comparison between numerical calculations and experimental results from Rocco (1996). Apparently, the effect of including diffuse cracking in marginal. In particular, the influence on the peak load never exceeds 1.2% of the value computed with the standard cohesive crack model.

4.2 *Splitting test specimens*
Figure 8 shows the calculated values of the peak load and the experimental results of Rocco (1999). Both numerical models give very similar results. There is only a small difference when $D/l_{ch} = 0.15$; the peak load is slightly lower for the diffuse crack model. The difference between the predictions of the models is greater for $b/D = 0.16$ than for $b/D = 0.08$.

The numerical results are in good agreement with the experimental results. The peak load predicted for

(a) $D/l_{ch} = 0.15$ $\bar{\varepsilon}^p E / f_t$
0.00
0.05
0.10
0.15
0.20
0.25

(b) $D/l_{ch} = 1.20$ $\bar{\varepsilon}^p E / f_t$
0.00
0.05

(c) $D/l_{ch} = 0.15$ $\bar{\varepsilon}^p E / f_t$
0.0
0.1
0.2
0.3
0.4
0.5

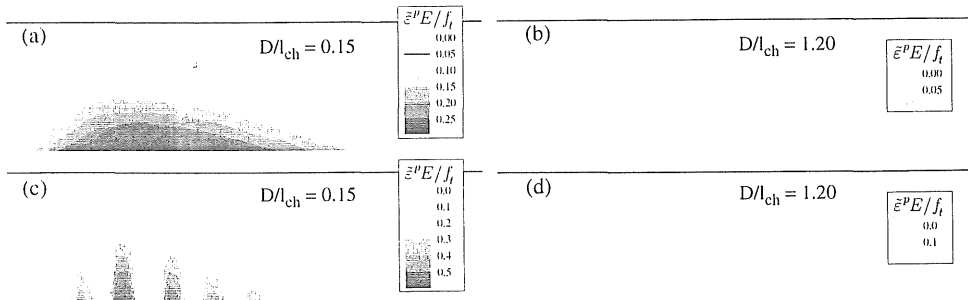(d) $D/l_{ch} = 1.20$ $\bar{\varepsilon}^p E / f_t$
0,0
0,1

Figure 6: Inelastic strain distributions for diffuse cracking on unnotched three-point-bend specimens. The figure shows the dark zone of figure 5 magnified.
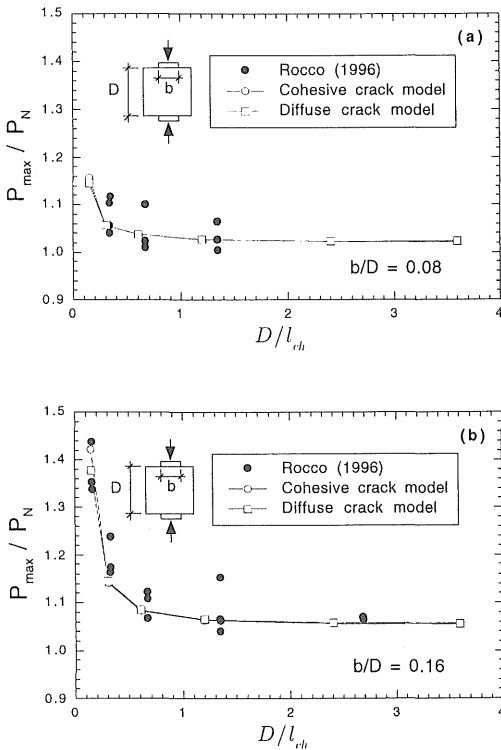

Figure 8: Peak load calculated with the cohesive crack model and the diffuse crack model and experimental results from Rocco(1996) for splitting test specimens: (a) $b/D = 0.08$; and (b) $b/D = 0.16$.

$D/l_{ch} = 0.15$ and $b/D = 0.16$ using the diffuse crack model is closer to the mean experimental peak load than the predicted using the standard cohesive model.

In view of these results, it seems that the diffuse cracking has a very little effect on the macroscopic response of the concrete splitting test specimens.

Figure 9 shows the distribution of diffuse cracking

on three different specimen sizes, including the smallest one, and the two widths of the bearing strip.

Diffuse cracking appears on two separated zones: (1) a narrow band along the main cohesive crack, and (2) a thin region on the top, near the end of the bearing strip. The latter zone grows in relative extent as the size of the specimen decreases. Only for $D/l_{ch} = 0.15$, the smallest size of specimen, the diffuse cracking is more intense here than near the main cohesive crack.

The width of material affected near the main cohesive crack is very narrow. The exception is again the smallest specimen, where the volume of affected bulk material is important (relative to the volume of the specimen).

The width of the bearing strip when $D/l_{ch} \geq 0.30$ has little influence on the process. When $D/l_{ch} = 0.15$, the wider the bearing strip, the smaller the volume of affected bulk material near the main cohesive crack.

At any rate, the extent of diffuse cracking is very small in all cases, which explains why diffuse cracking does not substantially affect macroscopic results, compared to the standard cohesive crack model, which neglects secondary cracking altogether.

5 CONCLUSIONS

1. Both versions of the diffuse crack model (non-softening and softening) are confirmed to be adequate to relieve the inconsistency of the standard cohesive crack model and to describe secondary cracking that must necessarily occur in specimens and structures failing through a single main crack.

2. For unnotched three-point-bend specimens, the diffuse cracking appears also on two wing-shaped zones on both sides of the specimen. For diagonal splitting specimens the diffuse cracking keeps distributed on two narrow strips at both sides of the main crack, at least until peak load is
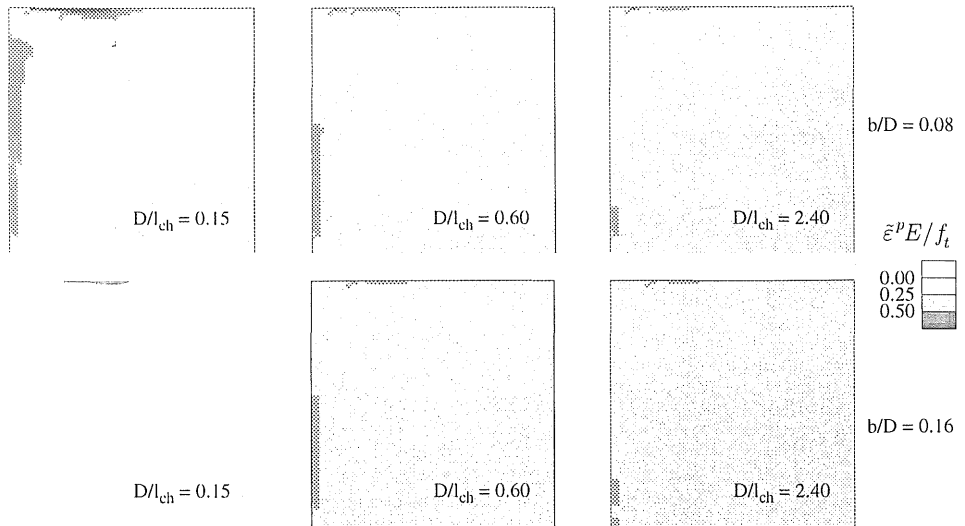
Figure 9: Inelastic strain distributions for diffuse cracking on splitting test specimens. Top row: $b/D = 0.08$; bottom row: $b/D = 0.16$

reached. A small zone of secondary cracking is detected at both sides of the load-bearing strips.

3. For unnotched three-point bend specimens a numerical difference appears between the diffuse cracking patterns according that a model with or without softening is used: numerical localization of diffuse cracking is seen when the softening model is used (although the actual localization is not measurable since it would correspond to an array of discrete microcracks with openings less than 0.1 microns). No localization has been detected for the diagonal-splitting test.

4. The splitting test is appropriate to ascertain the tensile strength of concrete if appropriate dimensions for specimens and bearing strips are selected. The propagation of the main cohesive crack is the key process and the importance of secondary cracking is negligible.

5. Both for three-point-bend unnotched beams and for diagonal-splitting specimens, the mechanical response is affected only slightly by the secondary cracking. The standard model (which is simpler and faster to use) can thus be used for most practical purposes

REFERENCES

Arbilla, I., Planas, J., Guinea G.V. & Elices, M. (2000). Effects of diffuse cracking around a cohesive crack. In *The 13th European Conference on Fracture (CD-ROM)*. Elsevier.

Barenblatt, G. (1962). The mathematical theory of equilibrium of cracks in brittle fracture. *Advances in Applied Mechanics* (7), 55–129.

Bazant, Z.P. & Planas, J. (1998). *Fracture and Size Effect in Concrete and Other Quasibrittle Materials*. CRC Press LLC.

Dugdale, D. (1960). Yielding of steel sheets containing slits. *Journal of Mechanics and Physics in Solids* (8), 10–108.

Elices, M. & Planas, J. (1989). Material models. In L. Elfgren (Ed.), *Fracture Mechanics of Concrete Structures*, pp. 16–66. Chapman and Hall.

Guinea, G. (1990). *Medida de la Energía de Fractura del Hormigón*. Ph. D. thesis, Dpto. Ciencia de Materiales, ETSI Caminos (UPM), Spain.

Hillerborg, A., Modeer, M. & Petersson, P. (1976). Analysis of crack formation and crack growth in concrete by means of fracture mechanics and finite elements. *Cement & Concrete Researchs* (6), 773–782.